Special Issue

Reactivity and Controlled Redox Reactions of Salt-like Intermetallic Compounds in Imidazolium-Based Ionic Liquids

Xian-Juan Feng,[a] Swantje Lerch,[b] Harry Biller,[b] Maik Micksch,[b] Marcus Schmidt,[a] Michael Baitinger,[a] Thomas Strassner,[b] Yuri Grin,[a] and Bodo Böhme*[a]

Substituted imidazolium ionic liquids (ILs) were investigated for their reactivity towards $Na_{12}Ge_{17}$ as a model system containing redox-sensitive *Zintl* cluster anions. The ILs proved widely inert for imidazolium cations with a 1,2,3-trisubstitution at least by alkyl groups, and for the anion bis(trifluoromethylsulfonyl)-azanide (TFSI). A minute conversion of $Na_{12}Ge_{17}$ observed on long-time contact with such ILs was not caused by dissolution of the salt-like compound, and did thus not provide dissolved Ge clusters. Rather, a cation exchange led to the transfer of Na^+ ions into solution. In contrast, by using benzophenone as an oxidizer, heterogeneous redox reactions of $Na_{12}Ge_{17}$ were initiated, transferring a considerable part of Na^+ into solution. At optimized conditions, an X-ray amorphous product $NaGe_{6.25}$ was obtained, which was thermally convertible to the crystalline type-II clathrate $Na_{24-\delta}Ge_{136}$ with almost completely Na-filled polyhedral cages, and α-Ge. The presented method thus provides unexpected access to $Na_{24-\delta}Ge_{136}$ in bulk quantities.

1. Introduction

Redox reactions of intermetallic compounds by using the inherent reactivity of CH acidic quaternary ammonium tetrahalogenido-aluminate ionic liquids have provided access to crystalline metastable allotropes such as Ge(*cF*136)[1] or Ge-(*oP*32).[2] Moreover, amorphous intermetallic phases like Zn_2Si_5[3] or intermediate products KGe_x[4] have been obtained, where the latter was convertible into the metastable type-II clathrate $K_{8.6}Ge_{136}$ by thermal treatment. The key challenge for such conversions has been to control the reactions of the ILs towards the sensitive precursors. With an immediate start of the redox conversion on contact, a possible dissolution of cluster anions like $[Ge_9]^{4-}$ in the IL as suggested for other group-14 anions in salt melts,[5] and their controlled oxidation in solution as known for respective ammonia or amine solutions[6,7] seems not feasible by principle. The reactions have thus been concluded to proceed essentially heterogeneously.[3,8–10] The key processes determining the redox behavior towards Zintl phases have been elucidated to be the removal of protic hydrogen atoms at the α- or β-carbon atoms of methyl- or longer alkyl chains of the quaternary ammonium ions by, e.g., strongly basic germanide anions. The initially formed hydride species on the surface finally decompose under liberation of H_2.[3] The quaternary ammonium ions in parallel undergo a Hofmann elimination via mechanisms depending on the place of proton abstraction.[1,9] Alternatively, nucleophilic substitution of alkyl chains by, e.g., germanide anions may occur, and the following decomposition of the intermediate germanium-alkyl surface species by disproportionation to alkanes and terminal alkenes, or a Wurtz-like coupling reaction to the respective alkanes leaves the oxidized final germanium-based product.[9,10]

The development of derivative heterogeneous gas-solid reactions succeeded in the preparation of a number of metastable intermetallic clathrates.[10–13] Here, the key redox processes such as the reaction of the precursors with hydrogen chloride or alkyl chlorides are equivalent to the above-discussed ones for precursors in direct contact with quaternary ammonium ions in the ILs. The respective oxidizers may even be generated in-situ by, e.g., chloride-induced thermal decomposition of quaternary ammonium ILs via Hofmann elimination or nucleophilic substitutions.[10] In that case, the liberated oxidizers have been concluded to also play an increasing role towards higher temperature for reactions with direct contact of the precursor with the ILs, for which self-decomposition becomes increasingly relevant.[8] With the gas-solid reactions, several disadvantages of the quaternary ammonium ionic liquids such as the limited thermal stability leaving hardly removable by-products for reactions at high temperature, the hardly controllable redox process itself or the occasionally challenging separation of sensitive solid products have been

[a] Dr. X.-J. Feng, Dr. M. Schmidt, Dr. M. Baitinger, Prof. Yu. Grin, Dr. B. Böhme
Max-Planck-Institut für Chemische Physik fester Stoffe
Abteilung Chemische Metallkunde
Nöthnitzer Straße 40
01187 Dresden (Germany)
E-mail: bodo.boehme@cpfs.mpg.de
[b] S. Lerch, H. Biller, Dr. M. Micksch, Prof. Dr. T. Strassner
Technische Universität Dresden
Fachrichtung Chemie und Lebensmittelchemie
Professur für Physikalische Organische Chemie
01062 Dresden (Germany)

Supporting information for this article is available on the WWW under https://doi.org/10.1002/open.202000262

Special Issue *An invited contribution to a Special Issue dedicated to Material Synthesis in Ionic Liquids.*

circumvented. On the other hand, ILs may provide favorable dissolution properties for ionic compounds, so that halogenide salts forming as co-products of the redox reactions may be dissolved,[3] and passivation effects[13] may thus be avoided. Moreover, type-II clathrate nanocrystals extracted from the quaternary ammonium ILs after crown-ether assisted reaction of, e.g., K_4Ge_9 may even indicate redox processes of chemically or colloidally dissolved species,[14] which still motivates to overcome the limitation of inherent reactivity of the ILs to enable controlled reactions of Zintl cluster compounds in IL solutions. With respect to an increased stability against nucleophilic attack, imidazolium-based ILs might be suitable substitutes for quaternary ammonium ILs. However, as the widely applied 1,3-disubstituted imidazolium cations are CH acids, forming remarkably stable carbene species,[15] only imidazolium cations featuring also a substitution at the carbon atom in 2-position seem to be a reasonable choice.

In this work, accordingly 1,2,3-trisubstituted imidazolium ILs were synthesized and investigated for their reactivity towards polar intermetallic phases by using the model precursor $Na_{12}Ge_{17}$,[16] which contains two different redox-sensitive Zintl cluster anions $[Ge_9]^{4-}$ and $[Ge_4]^{4-}$, and which has been known as a suitable starting material for the heterogeneous redox-preparation of Ge(*cF*136)[1,10,17] as well as for its salt-like behavior and capability of forming amine or ammonia solutions of $[Ge_9]^{4-}$ cluster anions.[16]

2. Results and Discussion

2.1. Reactivity of 1,2,3-Trisubstituted Imidazolium ILs

An initial investigation on the reactivity towards $Na_{12}Ge_{17}$ was performed for two 1,2,3-trisubstituted imidazolium ILs featuring the bis(trifluoromethylsulfonyl)azanide (bis(trifluoromethane)-sulfonimide) anion $[TFSI]^-$: 1-phenyl-2,3-dipropyl-imidazolium [TFSI] and 1,3-dibutyl-2-methyl-imidazolium [TFSI] (Figure 1).

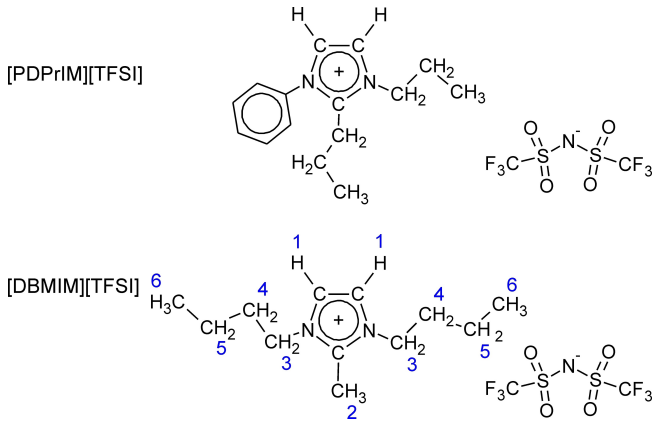

Figure 1. Structural formulas of the applied 1,2,3-trisubstituted imidazolium ILs. The blue numbering for the hydrogen atoms of the $[DBMIM]^+$ cation corresponds to the signal assignment in the ^1H NMR spectrum of that IL (Figure 4a).

In the following, the abbreviations [PDPrIM][TFSI] and [DBMIM][TFSI] will be used. Both ILs showed a remarkable inertness, so that $Na_{12}Ge_{17}$ remained widely unreacted even after long-time exposure of 14 days at 70 °C. X-ray powder diffraction (XRPD) detected the typical low-angle reflections of $Na_{12}Ge_{17}$ associated with an ordered arrangement of the $[Ge_9]^{4-}$ and $[Ge_4]^{4-}$ cluster entities in the visually unchanged dark-grey solid (Figure 2). In agreement with the reduced crystallinity of the $Na_{12}Ge_{17}$ phase, in both ILs a weak signal at about −12 ppm was detected in ^{23}Na NMR (Figure 3), suggesting the transfer of Na^+ ions from the solid $Na_{12}Ge_{17}$ precursor to the IL phase. The observed signal shift is well in agreement with that reported for Na^+ cations of Na[TFSI] in resembling IL solutions[18] and in the measured reference sample. In the pure ILs before contact with $Na_{12}Ge_{17}$, sodium was not detected by ^{23}Na NMR as exemplified for [DBMIM][TFSI] (Figure 3).

In order to facilitate a quantitative evaluation of the Na^+ transfer into the ILs, to elucidate the underlying reaction of $Na_{12}Ge_{17}$, and to study a possible co-dissolution of Ge species into the ILs a scale-up of the reaction mixtures was required. Since a significant difference in the reactivity of the two above-discussed ILs towards $Na_{12}Ge_{17}$ had not been evidenced, all further investigations were performed by using [DBMIM][TFSI] as a model system, the synthesis of which in suitable quality and quantity is less demanding (see Experimental Section).

2.2. Purity and Thermal Behavior of [DBMIM][TFSI]

With the method described in the experimental section, [DBMIM][TFSI] was obtained free of impurities as evidenced by ^1H NMR, chemical analysis and combined thermogravimetry-mass spectroscopy (TG-MS). In ^1H NMR, all observed signals were assigned to the protons of $[DBMIM]^+$ cations (Figures 1, 4a). The relative integrated intensities of the individual signals agreed with the expected molar ratio of the respective proton species (Table 1, sample a). Chemical analysis was in reasonable

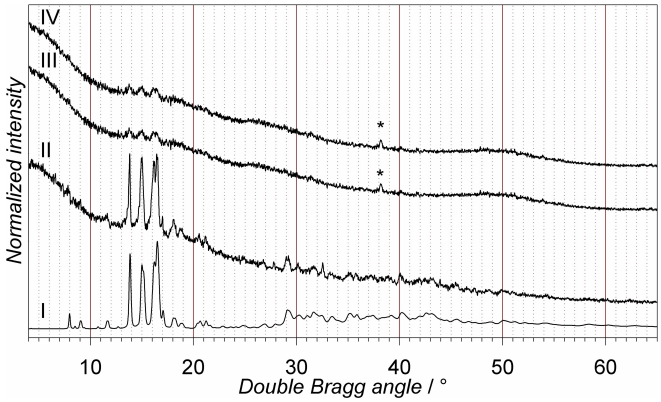

Figure 2. X-ray powder diffraction patterns of $Na_{12}Ge_{17}$ as calculated from Ref. [16] (I) and as experimentally observed before contact with an IL (II), and of the solids separated from [PDPrIM][TFSI] (III) and [DBMIM][TFSI] (IV) after contact at 70 °C for 14 days. The reflections marked with an asterisk are assigned to the strongest reflection of NaOH,[19] which likely formed due to hydrolysis during the measurement.

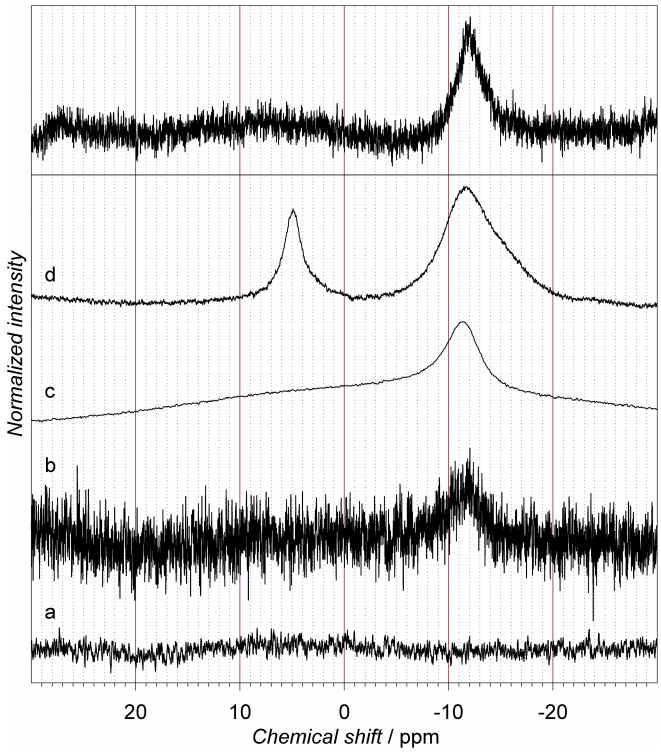

Figure 3. ^{23}Na NMR spectra for samples containing the ILs [PDPrIM][TFSI] (top diagram) and [DBMIM][TFSI] (bottom diagram) after different treatment. For [PDPrIM][TFSI], the sample was measured after contact with $Na_{12}Ge_{17}$ for 14 days at 70 °C. For the spectra of [DBMIM][TFSI]-based material the labels are chosen according to all further investigations throughout the paper: the pure IL (a), after contact with $Na_{12}Ge_{17}$ at 70 °C for 14 days (b), with dissolved Na[TFSI] in an about 1:13 molar ratio (c), and after reaction of $Na_{12}Ge_{17}$ with admixed benzophenone at 70 °C for 3 days (d). For the [DBMIM][TFSI] spectra (a) and (b), the noise level was reduced after normalization by applying a gliding average over 29 datapoints, corresponding to shift intervals of 0.021 ppm and 0.085 ppm, respectively.

Table 1. Relative integrated intensity of the $[DBMIM]^+$ ^{1}H-NMR signals.[a]

Signal / Sample	1	2	3	4	5	6	$\Sigma_{3,4,5,6}$
a	2.029	3	3.960	4.018	3.907	6.044	17.928
b	2.047	3	3.975	4.039	3.738	6.135	17.887
c	2.017	3	3.947	4.005	3.846	5.983	17.782
d	2.690[b]	3	4.119	4.093	4.082	6.249	18.543[b]
e[c]	1.980	3	3.973	4.000	3.924	5.850	17.747

[a] The samples are named and the signals are numbered according to the spectra shown in Figure 4. Signal 2 is arbitrarily assigned the ideal value of 3 corresponding to the number of respective hydrogen atoms in a $[DBMIM]^+$ cation (Figure 1). [b] The signal evidently comprises contributions of reaction products or residuals of benzophenone. [c] The spectrum (Figure 4e) shows three well-resolved further signals between 6.9 ppm and 7.2 ppm, which are assigned to benzophenone $(C_6H_5)_2CO$ with the expected 2:1:2 integrated intensity ratios and sum up to a total integrated intensity of 0.776 with the table normalization to signal 2.

agreement with the expected values (Experimental Section). In ^{19}F NMR, only one signal of the $[TFSI]^-$ anion was observed as expected (Figure S1).

TG-MS showed a significant mass-loss only above 250 °C (Figure 5), which comes along with a detectable contribution of organic fragment signals in the mass spectra. At lower temperature, the mass spectra contained the predominant signals of the argon purging gas with its three isotopes ^{36}Ar, ^{38}Ar and ^{40}Ar (Table 2). Weak additional signals were assigned to residual traces of H_2O, CO_2 and N_2 in the purging gas (see Supporting Information), so that the IL specimen actually did not contain detectable amounts of water or other impurities liberated below 250 °C. The mass loss of the [DBMIM][TFSI] sample above 250 °C showed an exponential development with steadily growing temperature (Figure 5). With a steady stream of the purging gas, such behavior suggests an exponential increase of the vapor pressure over the sample as a result of an evaporation equilibrium involving essentially only one single process. In the mass spectra, the eye-catching signal occurring in parallel is $m/z = 195$, which may be assigned to non-fragmented $[DBMIM]^+$ cations. Moreover, conclusive strong fragment-ion peaks were detected at $m/z = 57$ and $m/z = 56$, which should result from different fragmentation processes of the $[DBMIM]^+$ cations (Table 2). At higher temperature and, thus, larger partial pressure of sample vapor in the gas phase, also fragment ions including the imidazolium core were detected at $m/z = 138$ and $m/z = 80$. In parallel to the fragment-ion peaks assigned to the $[DBMIM]^+$ cations, conclusive cationic fragments tracing back to the $[TFSI]^-$ anions were detected. The investigation by TG-MS thus indicates that [DBMIM][TFSI] does not develop a detectable vapor pressure below 250 °C and does not decompose with significant rate. Above 250 °C, most likely [DBMIM][TFSI] ion pairs evaporate, because the $[DBMIM]^+$ cations are detected as non-dissociated entities in the gas

Table 2. Assignment of peaks in the mass spectra recorded for a [DBMIM][TFSI] sample in parallel to a thermogravimetric investigation.

m/z/u	(Fragment) Ion	Origin
Signals present already at $T < 250$ °C		
2	He^+	He in Ar
13.33	$^{40}Ar^{3+}$	Ar
16	O^+	CO_2 and H_2O traces in Ar purging gas
17	$[OH]^+$	H_2O traces in Ar purging gas
18	$^{36}Ar^{2+}$, $[H_2O]^{\cdot+}$	Ar and H_2O traces in Ar purging gas
19	$^{38}Ar^{2+}$	Ar
20	$^{40}Ar^{2+}$	Ar
28	$[CO]^{\cdot+}$, $[N_2]^{\cdot+}$	CO_2 and N_2 in Ar purging gas
36	$^{36}Ar^+$	Ar
38	$^{38}Ar^+$	Ar
40	$^{40}Ar^+$	Ar
44	$[CO_2]^{\cdot+}$	CO_2 in Ar purging gas
Characteristic signals at $T > 250$ °C occurring in connection with a mass loss of the sample		
195	$(C_4H_9)_2[(C_3H_2N_2)(CH_3)]^+$	$[DBMIM]^+$
138	$(C_4H_9)[(C_3H_2N_2)(CH_3)]^{\cdot+}$	$[DBMIM]^+$
133	$[SO_2CF_3]^+$	$[TFSI]^-$
110	$[(OS)_2N]^+$	$[TFSI]^-$
80	$[(C_3H_2N_2)(CH_2)]^{\cdot+}$	$[DBMIM]^+$
69	CF_3^+	$[TFSI]^-$
64	$[SO_2]^{\cdot+}$	$[TFSI]^-$
57	$[C_4H_9]^+$	$[DBMIM]^+$
56	$[C_4H_8]^{\cdot+}$	$[DBMIM]^+$
50	$[CF_2]^{\cdot+}$	$[TFSI]^-$
48	$[SO]^{\cdot+}$	$[TFSI]^-$

phase.[20] Any chemical decomposition reaction and the evaporation of the respective decomposition products was not expected to yield unspoiled $[DBMIM]^+$ cations. On the other hand, the detection of a "molecular ion" peak of any ion aggregate, i.e. the detection of cationic entities such as, $\{[DBMIM][TFSI]\}^+$ with $m/z = 475$ cannot be expected either. In agreement with that, signals in the range of $195 < m/z < 512$ were not detected.

To summarize, the investigations by ^{1}H NMR, chemical analysis and TG-MS confirm that [DBMIM][TFSI] as further used for all experiments with $Na_{12}Ge_{17}$ was free of detectable impurities. Moreover, any self-decomposition process at below 100 °C is unlikely even on long-term reactions. Any products of a self-decomposition thus cannot contribute to a conversion of $Na_{12}Ge_{17}$ in contact with [DBMIM][TFSI].

2.3. Quantitative Investigation of $Na_{12}Ge_{17}$ and [DBMIM][TFSI] After Long-Time Contact

After contact of [DBMIM][TFSI] with $Na_{12}Ge_{17}$ for 14 days at 70 °C, chemical analysis of the separated IL revealed the presence of sodium with a concentration of 10 mmol/l in the liquid phase. Germanium, in contrast, was detected only with negligible concentration (Table 3), so that the molar ratio of *n*(Na):*n*(Ge) observed in the IL was about 710:1. Therefore, $Na_{12}Ge_{17}$ does not dissolve in a salt-like manner in [DBMIM][TFSI] at the applied conditions. This holds for any feasible partial dissolution concerning distinct Ge cluster species only, as it was observed for ammonia or amine solvents before.[16] Preparative usage of any Ge species at such low concentration seems not feasible.

Considering the amount of the set-in $Na_{12}Ge_{17}$ precursor (400 mg, 0.26 mmol) and of the IL (12 g, 11 ml, 25.3 mmol), only about 3.5 % of the available sodium in $Na_{12}Ge_{17}$ (0.11 mmol out of 3.12 mmol) has been transferred to the liquid phase within the 14 days of contact. Such a low value is consistent with the inert behavior of the IL deduced from the XRPD investigation of $Na_{12}Ge_{17}$ (Figure 1). A possible solubility limit of Na[TFSI] in the IL as the reason for this quite low Na concentration may be ruled out: The detected Na^+ concentration translates into a molar ratio $n(Na^+):n([DBMIM]^+) \approx 1:230$ in the IL solution. In contrast, the homogeneous solution of Na[TFSI] in [DBMIM][TFSI] used as a reference for ^{23}Na NMR (Figure 3d), was about 18 times as concentrated ($n(Na^+):n([DBMIM]^+) \approx 1:13$.

Two principle ways seem feasible for the observed transfer of sodium from $Na_{12}Ge_{17}$ into the IL: A simple ion exchange reaction of Na^+ against $[DBMIM]^+$, which does not affect the germanide cluster anions, or a redox process of the $[Ge_9]^{4-}$ or $[Ge_4]^{4-}$ anions, leading to decomposition of the IL and to the release of the stoichiometric equivalent of Na^+ cations into the IL. In order to elucidate the predominant mechanism, more detailed investigations by using ^{1}H NMR of the IL phase were performed.

After contact of [DBMIM][TFSI] with $Na_{12}Ge_{17}$, slight changes of the chemical signal shifts occurred in the ^{1}H NMR spectrum, which come along with signal splits of the singlet signals 1 and 2, and with distinct broadening or a lack of resolution of the multiplet signals (Figures 4a, b). However, significant changes in the relative integrated signal intensities were not revealed (Table 1), and additional signals with stronger shift deviations were not observed. The slight deviations from ideal relative integrated intensities is rather caused by the unavoidable integration of satellite signals due to ^{13}C coupling, which may not univocally be assigned to a particular signal. Moreover, such satellite signals are also subject to broadening and changes in their chemical shift, which influences the assignment of the baseline as well. As a more robust measure, the sum of the integrated signals originating from the aliphatic hydrogen atoms of the butyl chains in $[DBMIM]^+$ was evaluated. This sum was found constant within ca. 0.2 % of its absolute value (Table 2). Significant decomposition of the $[DBMIM]^+$ cations on contact with $Na_{12}Ge_{17}$ was thus not indicated, as this would be expected to lead to detectable changes in the intensity ratios and to additional signals, particularly of hydrogen atoms connected to or with close distance to the aromatic core. Still, a decomposition level less than a percent, as it would expectedly be related to the observed low sodium content in the IL, might hardly be detectable in ^{1}H NMR. On the other hand, simple admixture of Na[TFSI] to [DBMIM][TFSI] (Figure 4c) had a similar effect on the ^{1}H NMR signals as the contact of the IL with $Na_{12}Ge_{17}$ (Figure 4b). Particularly, the observed chemical shifts had values similar to the changed signal components in the IL after contact with $Na_{12}Ge_{17}$ (Figure 4a–c). However, the Na concentration in the solution with admixed Na[TFSI] was distinctly larger, so that the ^{1}H singlet signals 1 and 2 of $[DBMIM]^+$ were sharp and completely shifted, and the multiplet signals were similarly sharp as in the pure IL [DBMIM][TFSI], and well-resolved. These results show that the presence of Na^+ ions in form of Na[TFSI] may largely explain the detected changes for the ^{1}H NMR signals in the IL after contact with $Na_{12}Ge_{17}$. Still, it seems surprising that the low Na^+ concentration detected by chemical analysis in the IL after contact with $Na_{12}Ge_{17}$ may influence such a large fraction of the $[DBMIM]^+$ cations.

Table 3. Chemical analysis of the IL [DBMIM][TFSI] after contact with $Na_{12}Ge_{17}$ and of the [DBMIM][TFSI]-benzophenone mixture after reaction with $Na_{12}Ge_{17}$: c_w is the mass concentration in the IL phase as revealed by chemical analysis; c_m and R_m are the calculated molar concentration and the molar ratio of Na^+ and $[DBMIM]^+$ in the IL solution phase, respectively.

Reaction conditions (sample label[a])	Element	c_w/mg l^{-1}	c_m/mmol l^{-1}	R_m[b]
pure IL $t = 14$ d $T = 70$ °C (sample b)	Na Ge	≈230 ≈1	10.0 0.014	≈1:230 –
IL + benzophenone $t = 3$ d $T = 70$ °C (sample d)	Na Ge	≈4000 ≈25	174 0.34	≈1:12.6 –

[a] The samples are labelled in accordance with Figures 3 and 4. [b] $R_m = n(Na^+)/n([DBMIM]^+)$ is calculated considering the applied volume of V(IL) = 11 ml and V(IL + benzophenone) = 11.5 ml as well as the observed density of ρ(IL) ≈ 1.1 g ml^{-1}, which is assumed to be unchanged for the Na containing solution phase as well as for the mixtures with benzophenone.

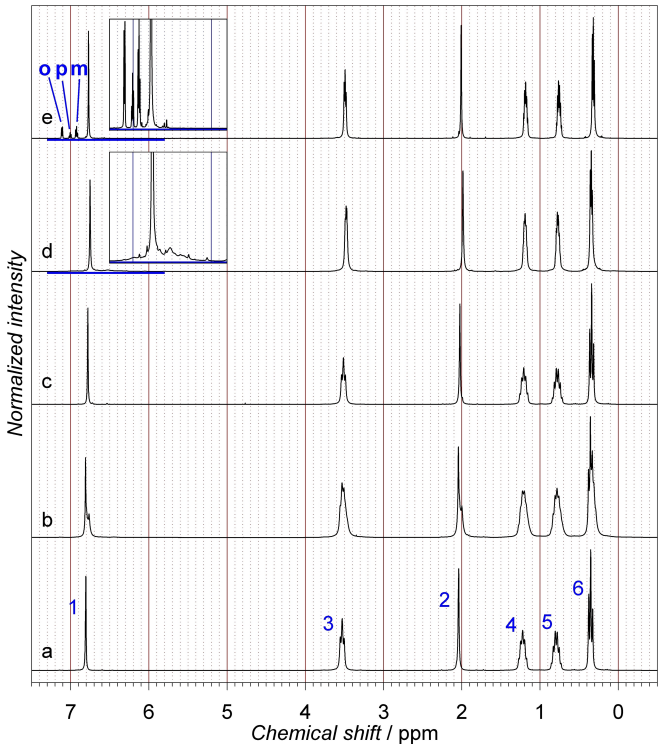

Figure 4. ^{1}H NMR spectra of the IL [DBMIM][TFSI] in pure form (a), after contact with $Na_{12}Ge_{17}$ at 70 °C for 14 days (b), with dissolved Na[TFSI] in an about 1:13 molar ratio (c), after reaction of $Na_{12}Ge_{17}$ with dissolved benzophenone at 70 °C for 3 days (d), and with dissolved benzophenone before contact with $Na_{12}Ge_{17}$ (e). The signal labels refer to the hydrogen atom labels in the structural formula of $[DBMIM]^+$ ions in Figure 1, the signals of benzophenone, $(C_6H_5)_2C{=}O$, in spectrum (e) are labelled according to the ortho- (o), meta- (m) and para- (p) position of the H atoms in the phenyl groups; blue underlines indicate the shift range featuring perceptible broad signal contributions of benzophenone or its reaction products in spectrum (d) and provide the respective reference in spectrum (e), which both are plotted with an about 10× zoomed-in intensity scale as inset graphs.

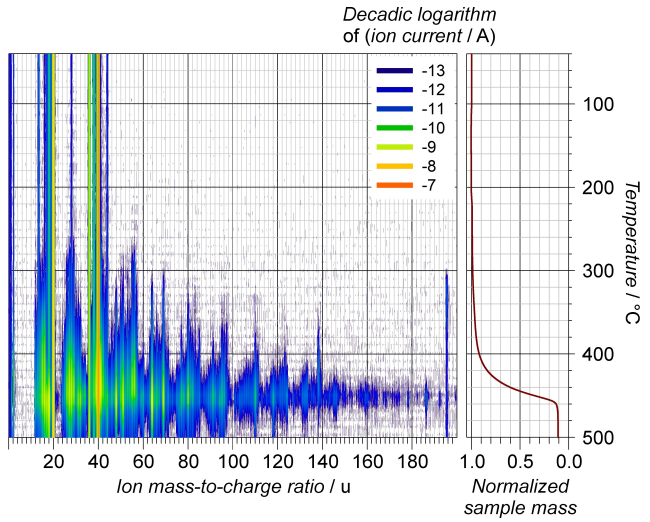

Figure 5. TG-MS investigation of [DBMIM][TFSI] with the development of the normalized sample mass with temperature on the right and the simultaneously recorded mass spectrum on the left. The ion current *I* of the measured mass spectra is color coded according to the given logarithmic scale.

However, it has been known from resembling imidazolium-based [TFSI]-ILs that the small and hard Na^+ cations, particularly if compared to the imidazolium cations with delocalized charge, feature a coordination by several $[TFSI]^-$ anions.[18] This may be expected to have a distinct impact on the IL solution already at low concentration, causing the formation of ion aggregates, in which the individual, originally chemically and magnetically equivalent protons of any structure fragment in the imidazolium cations may easily lose their magnetic equivalence. For a larger Na^+ concentration, on the other hand, the influence on the imidazolium cations should be more isotropic, so that magnetic equivalence is regained.

In consequence, the investigations suggest that the $[DBMIM]^+$ do not decompose in measurable amount on contact with $Na_{12}Ge_{17}$ at 70 °C for a time period of 14 days. The changes observed for the precursor as well as for the IL [DBMIM][TFSI] may reasonably be explained by a partial ion exchange of Na^+ against $[DBMIM]^+$ in the solid precursor phase under retention of the cluster anions, i.e. without detectable redox reaction. On the other hand, the highly charged $[Ge_4]^{4-}$ and $[Ge_9]^{4-}$ anions themselves are not transferred into the IL with relevant concentration. Performance of homogeneous redox reactions of the germanide cluster anions in [DBMIM][TFSI] without any suitable co-solvent is thus not feasible.

2.4. Dedicated Oxidation of $Na_{12}Ge_{17}$ in [DBMIM][TFSI] by Addition of Benzophenone

Benzophenone has long been known to be a suitably gentle oxidizer for the conversion of intermetallic phases.[21] For the conversion of $Na_{12}Ge_{17}$, a formal reaction according to Equation (1) was taken as the stoichiometric basis for the calculation of the set-in reactants.

$$Na_{12}Ge_{17} + 12\ (C_6H_5)_2CO \rightarrow 17\ Ge^0 + 12\ Na[(C_6H_5)_2CO^{\cdot}] \quad (1)$$

For 400 mg (0.26 mmol) of $Na_{12}Ge_{17}$, the respective equivalent of 570 mg (3.12 mmol) of benzophenone was used. Before starting the reaction, the miscibility of benzophenone and the IL [DBMIM][TFSI] was investigated. At 70 °C, the above amount of benzophenone (T_{melt} = 49 °C) and 11 ml (12 g, 25.3 mmol) of [DBMIM][TFSI] formed about 11.5 ml of a homogeneous liquid phase. A stoichiometric ratio of $n[(C_6H_5)_2CO]{:}n([DBMIM][TFSI])$ = 1:8.1 was thus achieved. After cooling of the mixture, besides the signals of [DBMIM][TFSI], the expected three signals of benzophenone were visible in the ^{1}H NMR spectrum as well-resolved doublet (ortho-), and triplets (meta- and para-positions of the phenyl groups) with the correct relative integrated intensities (Figure 4e, Table 1). However, the summed-up integrated intensity for all three benzophenone signals normalized to the integrated intensity of signal 2 of [DBMIM][TFSI] (Table 1) suggested a somewhat lower stoichiometric ratio of $n[(C_6H_5)_2CO]{:}n([DBMIM][TFSI])$ = 1:12.9 at room temperature. Actually, some colorless precipitate was observed in the speci-

men tube after NMR measurement, which may explain the deviant result. Accordingly, a saturated solution of benzophenone in the IL at room temperature should have a molar fraction of $x \approx 7\,\%$, provided that equilibrium had been reached.

On adding the above stoichiometric amount of powdered $Na_{12}Ge_{17}$ to the mixture of benzophenone and [DBMIM][TFSI] at 70 °C, the initially slightly yellowish liquid instantaneously turned via greenish to bluish, getting deeper colored by time. The coloring indicated the formation of the benzophenone radical anion[22] due to the reduction of benzophenone. The corresponding oxidation of $Na_{12}Ge_{17}$ led to a rapid depletion of sodium in the solid phase, as indicated by chemical analysis of the solid toluene-washed products obtained after different reaction times (Table 4). Apart from a low content of crystalline α-Ge, these products were X-ray amorphous (Figure 6). The α-Ge content was estimated to be on the order of 1 mass-% of the sample.

For the sample after a reaction time of 3 days, the liquid phase was exemplarily investigated by chemical analysis as well (Table 3). The observed sodium concentration in the liquid implied the presence of 46 mg of Na in the IL phase in total. In conclusion, about 2/3 of the sodium originally contained in the $Na_{12}Ge_{17}$ starting material have thus been transferred to the liquid phase. This roughly agrees with a remainder of about 1/4 of sodium in the solid phase (Table 4) as concluded from chemical analysis. Due to the investigation of different batches having slightly different gross conversion after the same reaction time, a slight discrepancy for the detected sodium amounts may arise. Complete analysis of solid and liquid of the same batch was hardly possible, however, because the separation by filtering, aiming at the complete recovery of the liquid, does not comply with a complete and impurity-free recovery of the fine-grained solid material (see experimental details). Nevertheless, it is evident that the oxidation by benzophenone comes along with the expected marked transfer of sodium into the IL phase.

Table 4. Chemical analysis of the solid phase remaining after reaction of $Na_{12}Ge_{17}$ with benzophenone in [DBMIM][TFSI] at 70 °C for the time *t*.

t/h	Element	*w*/mass-%	*n*(Na)/*n*(Ge)	*n*(Na)/n_0(Na)
0			1/1.42	1
6	Na	6.09(15)	1/4.34	0.33
	Ge	83.5(8)		
24	Na	5.02(4)	1/5.57	0.26
	Ge	88.3(7)		
72	Na	4.67(6)	1/6.25	0.23
	Ge	92.1(12)		

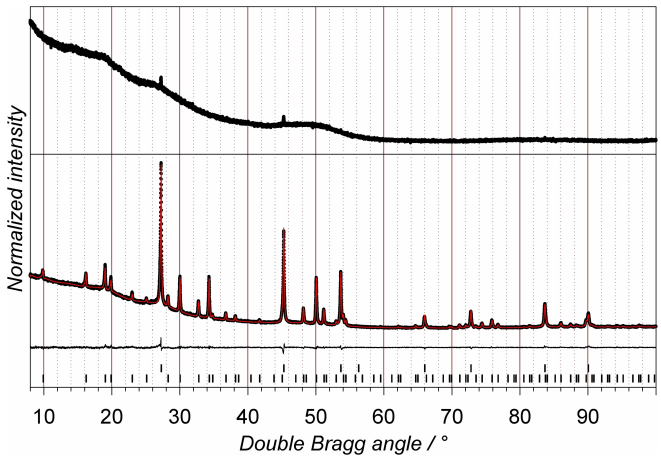

Figure 6. Experimental X-ray powder diffraction patterns: (top) the product obtained by oxidation of $Na_{12}Ge_{17}$ by benzophenone in [DBMIM][TFSI] at 70 °C for 3 days and subsequent washing with toluene; (bottom) the product after subsequent annealing in argon atmosphere at 340 °C for 18 hours. For the latter, the calculated pattern from Rietveld refinement is represented by a red line, and the difference of measured and calculated intensity is drawn below. The ticks in the bottom part mark the calculated positions of the Bragg reflections for α-Ge (top row) and Na_xGe_{136} with $x \approx 22$ (bottom row).

By ^{23}Na NMR, two well-resolved signals were detected in the IL phase after reaction (Figure 3d). The signal at about −12 ppm has a similar shift as assigned to Na^+ cations coordinated by TFSI anions before, i.e. experiencing a normal ionic environment. The asymmetric broadening might result from a number of slightly different coordination environments for Na^+. Most likely, the signal is thus associated to Na^+ coordinated by the diamagnetic benzopinacolate dianion resulting from the dimerization of benzophenone ketyl radical anions [Equation (2)]. As well, $[TFSI]^-$ coordination might occur. The dimerization of benzophenone radical anions may readily explain the vanishing color of the liquid phase on longer standing time after reaction under inert conditions.

$$2\ [(C_6H_5)_2CO^{\bullet}]^- \rightarrow [(C_6H_5)_2C(O) - C(O)(C_6H_5)_2]^{2-} \quad (2)$$

However, as the investigated liquid specimen was still colored at the time of NMR measurement, benzophenone radical anions should have been present as well. The second signal in the ^{23}Na NMR spectrum at about +5 ppm, featuring a distinct, likely paramagnetic, down-field shift,[23] is consequently concluded to originate from Na^+ cations, which are associated to the paramagnetic radical anions.

In ^{1}H NMR, on first glance the signals of benzophenone or derivative compounds seem to be absent after reaction with $Na_{12}Ge_{17}$ (Figure 4d). However, two broad signal groups tracing back to benzophenone become evident on careful analysis, which is in line with the observation of two distinct ^{23}Na signals. The first group is hidden in the background of the range around signal 1 of $[DBMIM]^+$ ions. The second signal is found to be covered by the multiplets of the aliphatic signals 3–6 showing a markedly enhanced integral intensity, if summed up (Table 1). Both additional signal contributions make up about 1.25 H atoms relative to 3 H-Atoms of signal 2 of the $[DBMIM]^+$ ions. Assuming that benzophenone is converted without loss of hydrogen atoms from the phenyl groups, the molar ratio of benzophenone plus its above-discussed conversion products to the $[DBMIM]^+$ cations is thus estimated to be 1:8. This result actually matches the nominal mixture of benzophenone and [DBMIM][TFSI] applied for the oxidation of $Na_{12}Ge_{17}$.

The benzophenone-based signals in the shift region around signal 1 of $[DBMIM]^+$ usually observed for protons on aromatic phenyl rings should be assigned to the protons in the above-dicussed pinacolate dianions, and eventually also to a contribu-

tion of residing benzophenone. Due to a variety of different coordination environments, the observed broadening seems explainable. The distinct high-field shift of the second set of signals suggests assignment to the benzophenone radical anions, for which the shift can be expected to be strongly altered by a combination of the paramagnetism of the unpaired electron and the negative ion charge, both experiencing delocalization over the π-system of the phenyl rings. In that case, the paramagnetism may also contribute to broadening of the signals, as a result of decreased relaxation time. Such an effect, although on smaller scale, may also be seen by the general trend to broader signals with hardly resolved multiplet signals for the whole sample. Moreover, broadening may arise also from the presence of a variety of dissolved species. To conclude, the findings of ^{23}Na NMR are in line with the result of ^{1}H NMR, both suggesting the presence of two distinctly different associate species of Na^+ with benzophenone and its monomeric or dimerized reduction products in the IL solution, which quantitatively fit the set-in stoichiometric ratio of the starting reaction mixture.

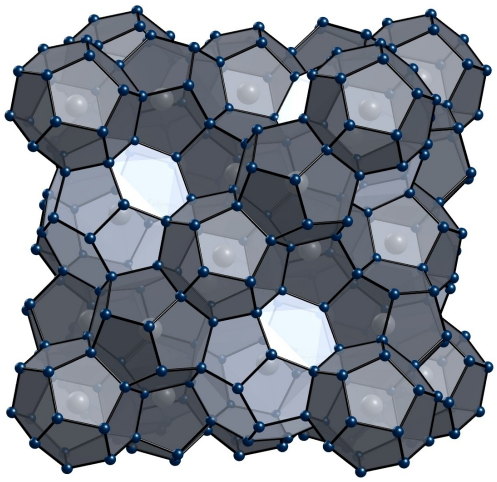

Figure 7. Type-II clathrate crystal structure[26] of $Na_{24-\delta}Ge_{136}$, in which covalently four-bonded Ge atoms (blue spheres) form a framework spanning pentagonal dodecahedral (dark grey) and hexakaidecahedral (light grey) cages, which are nearly completely filled by Na atoms (grey spheres).

2.5. Heat-Treatment of the X-Ray Amorphous Na-Ge Oxidation Products[24]

In order to study the thermal behavior of the X-ray amorphous oxidation products and to elucidate a possible conversion to potentially interesting materials as known for chemically related K–Ge phases,[4] annealing experiments were performed. Pre-investigations by differential thermal analysis had revealed several broad exothermic effects in the temperature range of $100\,^{\circ}C \leq T \leq 500\,^{\circ}C$, indicating a complex structural rearrangement behavior in the solid. In experiments using preparative amounts, particularly the product obtained by oxidation of $Na_{12}Ge_{17}$ with benzophenone in [DBMIM][TFSI] at 70 °C for 3 days was found to be suitable for a transformation into crystalline material containing the type-II clathrate phase $Na_{24-\delta}Ge_{136}$ (Figure 7).

A maximal yield of the clathrate phase was observed after annealing for 18 h at 340 °C. The product consisted, according to Rietveld refinement (Figure 6), of $Na_{24-\delta}Ge_{136}$ ($\delta \approx 2$) and α-Ge in a 45:55 mass ratio.[25] The crystalline phases were found to make up more than 90 mass-% of the sample,[24] showing that only a low mass fraction remained X-ray amorphous on annealing or undetected by XRPD. The clathrate phase had a lattice parameter of $a = 15.4355(4)$ Å.[24] This value is consistent with the composition deduced from Rietveld refinement, and conclusively only slightly smaller than the one observed for $Na_{23.0(5)}Ge_{136}$ ($a = 15.4412(7)$ Å), which was obtained only recently by an electrochemical oxidation at 280 °C.[17] As well, the value is close to other Na-rich compositions reported for that phase.[26–29] Remarkably, the temperature of 340 °C found to be optimal for the yield of $Na_{24-\delta}Ge_{136}$ is somewhat lower than the temperature range for a maximal yield of $Na_{24-\delta}Ge_{136}$ by rapid thermal degradation of bulk samples of Na_4Ge_4 at dynamic vacuum conditions (350 °C–380 °C).[26,30] Actually, transformation to the crystalline product in the present study also did not come along with a significant mass loss, which was found to be in the range of only 1%. Simple thermal degradation of the X-ray amorphous starting material with loss of Na may thus be excluded to be responsible for the formation of $Na_{24-\delta}Ge_{136}$. Rather, the X-ray amorphous product evidently recrystallizes to α-Ge and $Na_{24-\delta}Ge_{136}$ with hardly changing the overall sample composition. Apparently, there is a contradiction of that finding and the overall composition of the amorphous starting material (Table 4), suggesting almost exactly the refined clathrate composition for the whole sample, with the refined mass ratio of $Na_{22}Ge_{136}$ and α-Ge, which could be resolved by further detailed investigations. Finally, the sample fraction not detected by XRPD was revealed to contain a considerable part of the total sodium content in the sample by elaborate chemical analysis and investigations by ^{23}Na solid-state NMR.[24]

Having a phase contribution in the sample of above 40 mass-% and coming along with admixture of α-Ge as the only crystalline by-product, the preparation of $Na_{24-\delta}Ge_{136}$ from the X-ray amorphous oxidation products of $Na_{12}Ge_{17}$ with benzophenone seems to be a promising approach, particularly, if considering that thermal degradation processes and other methods so far have not been suitable to yield the phase in bulk quantities.[26–30] Also the recent more promising electrochemical approach so far has shown considerable and hardly removable contributions of Na_4Ge_{13}, α-Ge, Na-poor type-II clathrate $Na_{x\to 0}Ge_{136}$ and other rather unavoidable by-products.[17]

3. Conclusions

The 1,2,3-trisubstituted imidazolium-based ILs 1-phenyl-2,3-dipropyl-imidazolium [TFSI] and 1,3-dibutyl-2-methyl-imidazolium [TFSI] were obtained in high purity. At 70 °C, both ILs behave widely inert towards the particularly redox-sensitive salt-like intermetallic phase $Na_{12}Ge_{17}$. On longer contact times,

only a small fraction of the precursor is converted by the ILs, which, however, is due to a cation exchange reaction rather than to a redox process. Different to reactions known for that germanide in amine solvents or liquid ammonia, dissolution of $Na_{12}Ge_{17}$ with formation of preparative useful Zintl cluster anions does not occur in the ILs. By using benzophenone as a mild oxidizer, heterogeneous oxidation of $Na_{12}Ge_{17}$ at 70 °C in 1,3-dibutyl-2-methyl-imidazolium [TFSI] as the reaction medium yields X-ray amorphous $NaGe_x$ products. On heat treatment at optimally 340 °C, these products can be transformed into a widely crystalline product containing the intermetallic type-II clathrate phase $Na_{24-\delta}Ge_{136}$, and α-Ge as by-product. The X-ray amorphous material obtained from oxidation of $Na_{12}Ge_{17}$ with benzophenone is thus a promising precursor for the preparation of the hitherto difficult to access $Na_{24-\delta}Ge_{136}$ clathrate.

Experimental Section

General

For IL syntheses, tetrahydrofuran (Merck Millipore, reagent grade) and ethyl acetate (Sigma Aldrich, ACS reagent,) were used as received. Dry THF was obtained from a MBraun Compact solvent purification system. Methanol, CH_2Cl_2, $CHCl_3$, and pentane (technical grade) were purified by distillation. All other used chemicals were of reagent grade and were used without further purification.

Synthesis of 1-Phenyl-2,3-dipropylimidazolium bis(trifluoromethyl-sulfonyl)azanide ([PDPrIM][TFSI])

The preparation comprised three steps, the synthesis of 1-phenyl-2-propylimidazole (A1), the alkylation to 1-phenyl-2,3-dipropylimidazolium bromide (B1), and the subsequent ion exchange with Li[TFSI] (C1) (Scheme 1).

Step (A1): Magnesium turnings (8.79 g, 362 mmol, Merck KGaA, 99.5 %) were placed in a dried flask, rinsed with nitrogen and mixed with dry THF. Bromoethane (39.4 g, 362 mmol, Acros Organics, 99 %) in THF (50 mL) was added slowly and kept stirring until the magnesium chips were completely dissolved. The reaction was kept cool with an ice bath. Aniline (30.6 g, 329 mmol, Acros Organics 99.8 %) in THF (50 mL) was added slowly. Butyronitrile (25 g, 362 mmol, Sigma Aldrich, 99 %) was added after the gas evolution had subsided. After stirring overnight, the reaction was quenched with water. The aqueous phase was extracted with ethyl acetate (3×100 mL, distilled prior to use) and the combined organic phases were washed with distilled water (100 mL), saturated NaCl solution (100 mL) and dried with $MgSO_4$. The solvent was removed *in vacuo* and the residue dissolved in $CHCl_3$ (300 mL). Chloroacetaldehyde (40 mass-%, 51.7 g, 658 mmol) was added slowly, and the mixture was kept under reflux for 24 h. The solvent was removed *in vacuo* and the crude product dissolved in ethyl acetate (200 mL). The organic phase was washed twice with HCl solution (pH = 1, 100 mL) and the residue formed was filtered. NaOH pellets were added to the aqueous phase until a pH > 9 was reached. The aqueous phase was extracted with ethyl acetate (3×100 mL) and the combined organic phases were washed with saturated NaCl solution and dried over $MgSO_4$. The solvent was removed *in vacuo* and the crude product was purified through vacuum distillation (0.021 mbar, 100 °C). The product 1-phenyl-2-propyl-1*H*-imidazole was obtained as yellow oil (10.8 g, 68.5 mmol, 31 %). ^{1}H NMR ($CDCl_3$): δ/ppm = 7.53–7.39 (m, 3 H, H_{Ar}), 7.31–7.24 (m, 2 H, H_{Ar}), 7.06 (d, J = 1.41 Hz, 1 H, NCH), 6.97 (d, J = 1.41 Hz, 1 H, NCH), 2.61 (t, J = 7.93 Hz, 2 H, $NCCH_2$), 1.70 (sex., J = 7.93 Hz, 2 H, $NC(CH_2)CH_2$), 0.88 (t, J = 7.93 Hz, 3 H, CH_3). ^{13}C NMR ($CDCl_3$): δ /ppm = 148.5 (NCN), 137.9 (NC_{Ar}), 129.4 (C_{Ar}), 128.3 (C_{Ar}), 127.5 (C_{Ar}), 125.9 (C_{Ar}), 120.6 (C_{Ar}), 29.0 (CH_2), 21.4 (CH_2), 13.8 (CH_3). Elemental analysis calculated for $C_{12}H_{14}N_2$: C: 77.38 %, H: 7.58 %, N: 15.04 %, found: C: 77.17 %, H: 7.89 %, N: 15.35 %. Step (B1): In an Ace pressure tube, the imidazole (6.5 g, 34.9 mmol) was diluted with THF, and 1-bromopropane (4.72 g, 38.4 mmol, 1.1 eq.) was added. The reaction mixture was stirred at 90 °C for 24 h. The solvent was evaporated under reduced pressure and the crude product was washed with cold ethyl acetate and pentane. The procedure yielded 1-Phenyl-2,3-dipropylimidazolium bromide as white solid (9.1 g, 29.4 mmol, 84 %). ^{1}H NMR ($CDCl_3$): δ/ppm = 7.96 (d, J = 2.08 Hz, 1 H, NCH), 7.65–7.53 (m, 5 H, H_{Ar}), 7.35 (d, J = 2.08 Hz, 1 H, NCH), 4.33 (t, J = 7.83 Hz, 2 H, NCH_2), 3.04 (t, J = 7.83 Hz, 2 H, $NCCH_2$), 2.03 (sex., J = 7.83 Hz, 2 H, $N(CH_2)CH_2$), 2.48 (sex., J = 7.83 Hz, 2 H, $NC(CH_2)CH_2$), 1.07 (t, J = 7.83 Hz, 3 H, CH_3), 0.83 (t, J = 7.83 Hz, 3 H, CH_3). ^{13}C NMR ($CDCl_3$): δ/ppm = 147.4 (NCN), 134.6 (NC_{Ar}), 131.1 (C_{Ar}), 130.4 (C_{Ar}), 126.3 (C_{Ar}), 122.8 (C_{Ar}), 122.5 (C_{Ar}), 50.6 (CH_2), 26.3 (CH_2), 23.4 (CH_2), 21.1 (CH_2), 13.7 (CH_3) 11.1 (CH_3). Melting point: 59 °C. Elemental analysis calculated for $C_{15}H_{21}BrN_2$: C: 58.26 %, H: 6.84 %, N: 9.06 %. Found: C: 58.23 %, H: 6.75 %, N: 9.10 %. Step (C1): In a round bottom flask, the bromide salt (4.75 g, 15.3 mmol) was dissolved in methanol. Li[TFSI] (7.92 g, 19.3 mmol, 1.1 eq. in 70 % aqueous solution, ABCR, battery grade) and additional water were added to the reaction mixture. CH_2Cl_2 was added and the 2-phase system was stirred at room temperature for 24 h. The organic phase was separated and the aqueous phase was extracted two times with CH_2Cl_2. The combined organic phases were washed twice with water and dried over $MgSO_4$. The solvent was removed *in vacuo* to yield the liquid product (7.51 g, 14.7 mmol, 96 %). ^{1}H NMR ($CDCl_3$): δ/ppm = 7.66–7.57 (m, 3 H, H_{Ar}), 7.50–7.43 (m, 3 H, H_{Ar}), 7.29 (d, J = 2.17 Hz, 1 H, H_{Ar}), 4.17 (t, J = 7.57 Hz, 2 H, NCH_2), 2.89 (t, J = 7.57 Hz, 2 H, $NCCH_2$), 1.99 (sex., J = 7.57 Hz, 2 H, H_{Me}), 1.95 (sex., J = 7.57 Hz, 2 H, $N(CH_2)CH_2$), 1.54 (sex., J = 7.57 Hz, 2 H, $NC(CH_2)CH_2$), 1.08 (t, J = 7.57 Hz, 3 H, CH_3), 0.87 (t, J = 7.57 Hz, 3 H, CH_3). ^{13}C NMR ($CDCl_3$): δ/ppm = 147.1 (NCN), 134.3 (NC_{Ar}), 131.4 (C_{Ar}), 130.5 (C_{Ar}), 126.1 (C_{Ar}), 122.9 (C_{Ar}), 121.6 (C_{Ar}), 50.4 (CH_2), 25.4 (CH_2), 23.1 (CH_2), 20.9 (CH_2), 13.7 (CH_3) 10.9 (CH_3). ^{19}F NMR ($CDCl_3$): δ = −79.4. Elemental analysis calculated for $C_{17}H_{21}F_6N_3O_4S_2$: C: 40.04 %, H: 4.15 %, N: 8.25 %, S: 12.59 %, found: C: 40.28 %, H: 4.14 %, N: 8.38 %, S: 12.39 %.

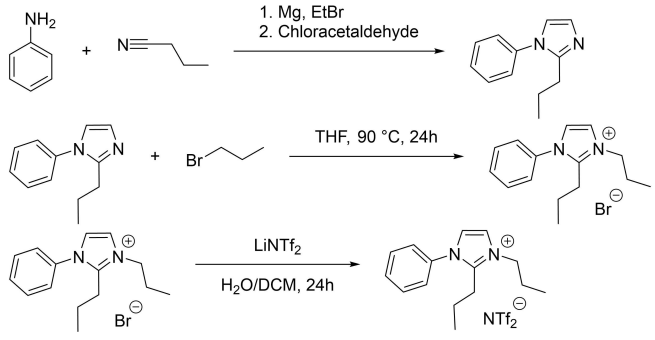

Scheme 1. Reaction sequence and conditions for the preparation of [PDPrIM][TFSI].

Synthesis of 1,3-Dibutyl-2-methylimidazolium bis (trifluoromethyl-sulfonyl)azanide ([DBMIM][TFSI])

The preparation comprised two steps, the synthesis of 1,3-dibutyl-2-methylimidazolium bromide (A2) and the subsequent ion exchange with Li[TFSI] (B2) (Scheme 2).

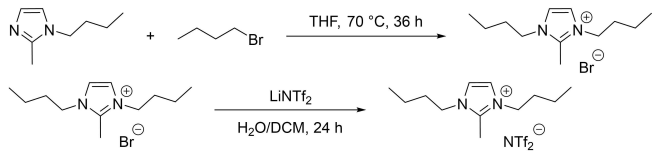

Scheme 2. Reaction sequence and conditions for the preparation of [DBMIM][TFSI].

Step (A2): In a 1 L round-bottom flask equipped with a pressure valve, 100 g of 1-butyl-2-methylimidazole (0.72 mol, synthesized according to the literature[31]) were dissolved in 250 mL THF, and butylbromide (111 g, 0.8 mol, 1.1 eq., ABCR, 98%) was added. The mixture was stirred at 70 °C for 6 h. After cooling to room temperature, the volatile compounds were evaporated under reduced pressure and the product was obtained as highly viscous yellow oil (196 g, 0.71 mol, 99%). ^{1}H NMR ($CDCl_3$): $\delta/ppm = 7.59$ (s, 2 H, H_{ar}), 4.25 (t, $J = 7.46$ Hz, 4 H, CH_2), 2.79 (s, 3 H, $CH_{3,ar}$), 1.71–1.85 (m, 4 H, CH_2), 1.36 (dq, $J_1 = 15.18$ Hz, $J_2 = 7.47$ Hz, 4 H, CH_2), 0.93 (t, $J = 7.37$ Hz, 6 H, CH_3). ^{13}C NMR (75 MHz, $CDCl_3$): $\delta/ppm = 143.0$ ($NC(CH_3)N$), 121.6 (NCHCHN), 48.8 (CH_2), 31.7 (CH_2), 19.6 (CH_2), 13.5 (CH_3,ar), 10.9 (CH_3). Elemental analysis calculated for $C_{12}H_{23}BrN_2 \cdot \times 0.1\ H_2O$: C: 51.61%, H: 8.64%, N: 10.62%. Found: C: 52.03%, H: 8.44%, N: 10.11%. Step (B2): In a 2 L round-bottom flask, 192 g of the 1,3-dibutyl-2-methyl-1H-imidazoliumbromide (0.7 mol) were dissolved in 100 mL methanol. Slowly, 315 g of a 70% aqueous solution of Li[TFSI] (0.77 mol, 1.1 eq, ABCR, battery grade) were added. Additional 300 mL of water and 300 mL of CH_2Cl_2 were added to obtain a clear organic and aqueous phase. The mixture was stirred at room temperature. After 24 h, the organic phase was separated and washed three times with water. The organic phase was dried over $MgSO_4$, filtered and the solvent was removed under reduced pressure. The obtained liquid was dried in high vacuum for 15 h. The product was obtained as pale yellow liquid (306 g, 0.64 mol, 92%) and subsequently stored over molecular sieve (3 Å, Merck) in an argon glovebox. ^{1}H NMR ($CDCl_3$): $\delta/ppm = 7.22$ (s, 2 H, H_{ar}), 4.07 (t, $J = 7.46$ Hz, 4 H, CH_2), 2.62 (s, 3 H, $CH_{3,ar}$), 1.72–1.86 (m, 4 H, CH_2), 1.38 (dq, $J_1 = 15.11$ Hz, $J_2 = 7.43$ Hz, 4 H, CH_2), 0.97 (t, $J = 7.37$ Hz, 6 H, CH_3). ^{13}C NMR ($CDCl_3$): $\delta/ppm = 143.0$ ($NC(CH_3)N$), 121.2 (NCHCHN), 119.8 (q, $J = 321.3$ Hz, CF_3), 48.6 (CH_2), 31.5 (CH_2), 19.5 (CH_2), 13.3 (CH_3,ar), 9.7 (CH_3). ^{19}F NMR ($CDCl_3$): $\delta/ppm = -79.5$ (Figure S1). Elemental analysis calculated for $C_{14}H_{23}F_6N_3O_4S_2$: C: 35.37%, H: 4.88%, N: 8.84%, S: 13.49%. Found: C: 34.99%, H: 4.51%, N: 9.07%, S: 13.72%.

Preparation of $Na_{12}Ge_{17}$

In an argon glovebox, a stoichiometric mixture of Na (ChemPur, Ingot, ampouled, 99.9%) and powdered Ge (ChemPur, Pieces, 99.9999 + %) was reacted in a sealed Ta ampoule by heating in an induction furnace to 1100 °C for 2 min. Afterwards, the sample was allowed to cool down to room temperature. According to XRPD, phase-pure material was obtained (Figure 2).

Reactivity Test of $Na_{12}Ge_{17}$ in the ILs

In an argon glovebox, $Na_{12}Ge_{17}$ (400 mg, 0.27 mmol) was powdered in a dry agate mortar and added to 11 ml of the ILs [PDPrIM][TFSI] or [DBMIM][TFSI], which were preheated to 70 °C in dried Duran-glass vessels. After stirring the samples for 14 days at that temperature, the powders were manually separated from the liquid, and investigated by XRPD. For further investigation, the IL phases were isolated by using a glass-fiber filter (Whatman), which had been vacuum-dried at 200 °C before usage. As a reference for ^{23}Na and ^{1}H, Na[TFSI] (Alfa Aesar, 99.8%) was admixed to [DBMIM][TFSI] in a 1 : 10 molar ratio.

Conversion of $Na_{12}Ge_{17}$ with Benzophenone in [DBMIM][TFSI]

In an argon glovebox, $Na_{12}Ge_{17}$ (400 mg, 0.27 mmol) was powdered in a dry agate mortar and added to a mixture of 11 ml (12 g, 25.3 mmol) [DBMIM][TFSI] and 570 mg (3.12 mmol) benzophenone, which had been preheated to 70 °C in a dried Duran-glass vessel. The reaction mixture was stirred at that temperature for the intended reaction time, and was subsequently allowed to cool down to room temperature. For isolating the IL phase, a glass-fiber filter was used. To obtain the solid phase, the mixture was allowed to settle, the supernatant IL phase was removed by a pipette, and the crude product with still adherent IL was 10 times washed with dry toluene (Sigma-Aldrich, anhydrous, 99.8%). This washing procedure was performed under argon atmosphere by using standard laboratory Schlenk equipment. After washing, the obtained dark-grey powder product was dried in vacuum at room temperature and subsequently stored in the argon glovebox.

Heat Treatment of the X-Ray Amorphous Oxidation Product from the Reaction of $Na_{12}Ge_{17}$ with Benzophenone in [DBMIM][TFSI]

In an argon glovebox, 130 mg of the oxidation product powder were filled into a dried Duran-glass crucible. The crucible was placed into a Duran-glass tube and inserted into a preheated and calibrated tube furnace. After the intended reaction time, the reactor was allowed to cool down to room temperature, and the obtained product powder was stored in the argon glovebox.

X-Ray Powder Diffraction (XRPD)

The air-sensitive specimens were fixed in an argon glovebox between two Kapton foils (Chemplex, 7.5 μm), and the XRPD data were recorded on air by using a Guinier Huber G670 camera (Cu $K\alpha_1$ radiation, $\lambda = 1.540598$ Å, germanium monochromator, image plate detector $5° \leq 2\theta \leq 100°$, $\Delta 2\theta = 0.005°$). For the refinement of lattice parameters and for the investigation of crystallinity, LaB_6 (NIST SRM 660a) standard was added to the specimen and used as a reference for reflection positions and reflection intensities. Lattice parameters were accordingly refined from reflection positions individually determined by profile deconvolution, and corrected by the standard reflections by using the WinCSD program package.[32] Rietveld refinement was performed by using JANA2006.[33] For the estimation of absolute mass-fractions of crystalline phases in the powder samples, the mass fractions from Rietveld refinement were referenced to the ratio of the refined mass fraction of LaB_6 standard to the expected one from specimen preparation.[24]

Nuclear Magnetic Resonance Spectroscopy (NMR)

For routine characterization of the synthesized IL samples or intermediate compounds, the specimens were dissolved in $CDCl_3$. ^{1}H (300 MHz) and ^{13}C (75 MHz) spectra were recorded on a Bruker AC 300 P, and ^{19}F (282 MHz) spectra on a Bruker AV III 600 spectrometer at room temperature. For the investigations related to the behavior of $Na_{12}Ge_{17}$ or the oxidation of that phase, IL samples were investigated without solvent, because any possible reaction with, e.g., $CDCl_3$ was to be excluded. In an argon glovebox, the IL specimens were filled into NMR sample tubes, a sealed capillary containing DMSO(D_6) was inserted, providing a small detectable signal for spectrum calibration, and the tube was sealed

air-tight afterwards. ^{1}H (300 MHz) spectra were likewise recorded on the Bruker AC 300 P spectrometer, ^{23}Na (159 MHz) spectra were recorded on the Bruker AV III 600 spectrometer. ^{1}H and ^{13}C NMR spectra were referenced internally by using the solvent residual signal of $CDCl_3$ (^{1}H: 7.26 ppm, ^{13}C: 77 ppm) and $(CD_3)_2SO$ (^{1}H: 2.50 ppm, ^{13}C: 39.5 ppm), respectively, while ^{19}F and ^{23}Na NMR spectra were referenced by external device standards.

Thermogravimetry Combined with Mass Spectroscopy (TG-MS)

The thermal decomposition behavior of [DBMIM][TFSI] was investigated by a combined TG-MS measurement using an inhouse-developed combination of a thermobalance (Netzsch STA 409 CD) and a quadrupole mass spectrometer (Pfeiffer Quadstar QMS 422, electron impact ionization at 70 eV, $0 < m/z < 512$), which was operated in an argon glovebox. About 5 mg of the IL were weighed in a dried and calibrated Al_2O_3 crucible, covered by a lid featuring a small bore, and transferred under protective conditions onto the TG-MS setup. The specimen was heated up to 800 °C with a heating rate of 5 K min^{-1}. During the whole heat treatment, the gases evolving from the specimen intermixed with a continuous argon purging-gas stream and were directed to the ionization chamber of the mass spectrometer by using a skimmer located directly above the bore of the reaction crucible. Background mass spectra were recorded and the thermobalance was calibrated before the measurement by using the same conditions.

Chemical Analysis

The sodium and germanium content of the X-ray amorphous oxidation products was determined by using inductively coupled plasma-optical emission spectrometry (ICP-OES, VISTA RL, Varian, matrix matched standard). The investigated specimens were digested in aqueous HNO_3/HF by a microwave assisted procedure (ETHOS plus 2, MLS) in closed Teflon containers. Routine elemental analysis (C, H, N, S) for the prepared ionic liquids and their intermediates was performed on a Hekatech EA 3000 Euro Vector elemental analyzer. The given values in percent are arithmetic means of two measurements.

Determination of Melting Points

As a routine characterization method for organic solids, the given melting points were determined by using a Wagner and Munz Polytherm hot stage microscope.

Acknowledgements

Funding by Deutsche Forschungsgemeinschaft within the Priority Program SPP1708 is gratefully acknowledged. We thank H. Borrmann, Yu. Prots and S. Hückmann for the recording of XRPD data, U. Schmidt, A. Völzke and G. Auffermann for chemical analyses, S. Scharsach for TG-MS experiments and M. Bobnar for helpful discussion.

Conflict of Interest

The authors declare no conflict of interest.

Keywords: intermetallic clathrates · ionic liquids · oxidation reactions · redox reactions · Zintl phases

[1] A. M. Guloy, R. Ramlau, Z. Tang, W. Schnelle, M. Baitinger, Yu. Grin, *Nature* **2006**, *443*, 320–323.
[2] Z. Tang, A. P. Litvinchuk, M. Gooch, A. M. Guloy, *J. Am. Chem. Soc.* **2018**, *140*, 6785–6788.
[3] X. Feng, B. Böhme, M. Bobnar, P. Simon, W. Carrillo-Cabrera, U. Burkhardt, M. Schmidt, U. Schwarz, M. Baitinger, T. Straßner, Yu. Grin, *Z. Anorg. Allg. Chem.* **2017**, *643*, 106–113.
[4] A. M. Guloy, Z. Tang, R. Ramlau, B. Böhme, M. Baitinger, Yu. Grin, *Eur. J. Inorg. Chem.* **2009**, 2455–2458.
[5] S. Wengert, R. Nesper, *J. Solid State Chem.* **2000**, *152*, 460–465.
[6] S. C. Sevov, J. M. Goicoechea, *Organometallics* **2006**, *25*, 5678–5692.
[7] S. Scharfe, F. Kraus, S. Stegmaier, A. Schier, T. F. Fässler, *Angew. Chem.* **2011**, 123, 3712–3754; *Angew. Chem. Int. Ed.* **2011**, *50*, 3630–3670.
[8] B. Böhme, M. Baitinger, S. Hoffmann, Yu. Grin in *Sci. Rep. 2009–2011*, Max-Planck-Institut für Chemische Physik fester Stoffe, Dresden, **2011**, pp.75–77.
[9] B. Böhme, *Neue Präparationswege für intermetallische Verbindungen*, PhD Dissertation, Technische Universität Dresden, **2010** (published in Logos, Berlin, **2010**).
[10] B. Böhme, S. Hoffmann, M. Baitinger, Yu. Grin, *Z. Naturforsch.* **2011**, *66b*, 230–238.
[11] B. Böhme, A. Guloy, Z. Tang, W. Schnelle, U. Burkhardt, M. Baitinger, Yu. Grin, *J. Am. Chem. Soc.* **2007**, *129*, 5348–5349.
[12] Y. Liang, B. Böhme, M. Reibold, W. Schnelle, U. Schwarz, M. Baitinger, H. Lichte, Yu. Grin, *Inorg. Chem.* **2011**, *50*, 4523–4528.
[13] B. Böhme, M. Bobnar, A. Ormeci, S. Peters, W. Schnelle, M. Baitinger, Yu. Grin, *Z. Kristallogr.* **2017**, *232*, 223–233.
[14] P. Simon, Z. Tang, W. Carrillo-Cabrera, K. Chiong, B. Böhme, M. Baitinger, H. Lichte, Yu. Grin, A. M. Guloy, *J. Am. Chem. Soc.* **2011**, *133*, 7596–7601.
[15] a) M. N. Hopkinson, C. Richter, M. Schedler, F. Glorius, *Nature* **2014**, *510*, 485–496; b) J. Arduengo III, M. Kline, R. L. Harlow, *J. Am. Chem. Soc.* **1991**, *113*, 361–363.
[16] W. Carrillo-Cabrera, R. Cardoso Gil, M. Somer, Ö. Persil, H. G. von Schnering, *Z. Anorg. Allg. Chem.* **2003**, *629*, 601–608.
[17] B. Böhme, *Inorg. Chem.* **2020**, *59*, 11920–11924.
[18] H. Yoon, H. Zhu, A. Hervault, M. Arman, D. R. MacFarlan, M. Forsyth, *Phys. Chem. Chem. Phys.* **2014**, *16*, 12350–12355.
[19] H. Jacobs, J. Kockelkorn, T. Tacke, *Z. Anorg. Allg. Chem.* **1985**, 119–124.
[20] a) S. D. Chambreau, G. L. Vaghjiani, A. To, C. Koh, D. Strasser, O. Kostko, S. R. Leone, *J. Phys. Chem. B* **2010**, *114*, 1361–1367; b) E. Anastasia, J. Varga, G. Matusvhek, M. R. Saraji-Bozorgzad, T. Denner, R. Zimmermann, P. Schmidt, *J. Phys. Chem. B* **2018**, 122, 8738–8749.
[21] A. Grüttner, R. Nesper, H. G. von Schnering, *Angew. Chem.* **1982**, *94*, 933.
[22] Römpp-Lexikon Chemie, 10. Auflage (Eds.: J. Falbe, M. Regitz), Georg Thieme Verlag, Stuttgart, **1996–1999** .
[23] H. Friebolin, Ein- und zweidimensionale NMR-Spektroskopie, 4. Auflage, Wiley-VCH, Weinheim, **2006** .
[24] The detailed information will be published elsewhere. Within the frame of this present paper, only the most striking results will be summarized.
[25] Structural information and results of Rietveld refinement[33] of the product after thermal treatment at 340 °C for 18 h ($R_{profile} = 0.015$): Phase I – $Na_{22}Ge_{136}$: Space group $Fd\bar{3}m$ (227, origin choice 2), $a = 15.4355(4)$ Å (obtained from individual reflection positions corrected with LaB_6 internal standard[32]), mass fraction: 44.2(8) %; Na1 at 16*c*, 0,0,0, $U_{iso} = 0.022(16)$ Å^2; Na2 at 8*b*, 3/8,3/8,3/8, $U_{iso} = 0.125$ Å^2, *occ* = 0.67(9); Ge1 at 8*a*, 1/8,1/8,1/8, $U_{iso} = 0.016(6)$ Å^2; Ge2 at 32*e*, 0.2182(4),*x*,*x*, $U_{iso} = 0.013(4)$ Å^2; Ge3 at 96 *g*, 0.0674(2),*x*,0.3715(4), $U_{iso} = 0.010(3)$ Å^2; R_{Bragg}(obs) = 0.042; Phase II–α-Ge: Space group $Fd\bar{3}m$ (227, origin choice 2), $a = 6.5551(2)$ Å (vs. LaB_6), mass fraction: 55.8(8)%; Ge at 8*a*, 1/8,1/8,1/8, $U_{iso} = 0.0131(11)$ Å^2; R_{Bragg}(obs) = 0.056. For the calculation of the estimated standard deviations (e.s.d.), a correction according to Bérar and Lelann[34] was applied, accounting for correlations in the profile fit by a factor, which was determined to be 5.2.
[26] P. Hagenmuller, R. Naslain, M. Pouchard, C. Cros, *Spec. Pub. Chem. Soc.* **1967**, *22*, 207–221.
[27] C. Cros, M. Pouchard, P. Hagenmuller, *J. Solid State Chem.* **1970**, *2*, 570–581.
[28] B. Böhme, M. Reibold, G. Auffermann, H. Lichte, M. Baitinger, Yu. Grin, *Z. Kristallogr.* **2014**, *229*, 677–686.

[29] T. Kume, T. Ban, F. Ohashi, H. S. Jha, T. Sugiyama, T. Ogura, S. Sasaki, S. Nonomura, *CrystEngComm* **2016**, *18*, 5630–5638.
[30] M. Beekman, J. Gryko, H. F. Rubin, J. A. Kaduk, W. Wong-Ng, G. S. Nolas, *24th International Conference on Thermoelectrics*, Clemson, SC, 2005; ICT, **2005**, pp. 234–237.
[31] A. R. Gholap, K. Venkatesan, T. Daniel, R. J. Lahoti, K. V. Srinivasan, *Green Chem.* **2003**, *5*, 693–696.
[32] L. Akselrud, Yu. Grin, *J. Appl. Crystallogr.* **2014**, *47*, 803–805.
[33] V. Petříček, M. Dušek, L. Palatinus, *Z. Kristallogr.* **2014**, *229*, 345–352.
[34] J.-F. Bérar, P. Lelann, *J. Appl. Crystallogr.* **1991**, *24*, 1–5.

Manuscript received: September 4, 2020
Revised manuscript received: December 1, 2020